

# Geant4 simulation for the digital electromagnetic calorimeter

Yoshinari Mikami\*

*University of Birmingham\*, Edgbaston Birmingham, UK*

On behalf of the CALICE UK digital ECAL team

1st Nov. 2011\*  
(Internal note)

## **Abstract**

We investigated the feasibility for the digital ECAL with Geant4 simulation. In this note, we will discuss some basic responses of the digital ECAL device at the Geant4 level. The geometry modification, the cell energy deposit, the cell size optimization, the linearity and the energy resolution are described here as the first test of the Geant4 response for the digital ECAL.

---

\* This note was summarized for the study at University of Birmingham during 2006 to 2008. Contact e-mail address now at [ymikami@cern.ch](mailto:ymikami@cern.ch)

This is an Internal Note. Material in this note is for the use of members of the CALICE UK MAPS group only, and should not be presented publicly.

## Introduction

We study for the digital ECAL (Electromagnetic CALorimeter) which measures the electromagnetic shower energy just by counting the numbers of secondary particles after the shower. The numbers of secondary particles are proportional to the energy of the incoming particle, therefore, we can measure the incident energy if we could obtain the precise number of secondary particles. This method requires a small cell size because we have to detect the secondary particles one by one. For this purpose, we use the Monolithic Active Pixel Sensor (MAPS) as the Si sensitive sensor of the digital ECAL. This CMOS sensor is not a pure silicon and it is widely used in other fields, therefore, this option can be cost-effective at least for its construction.

## Geometry

We use the ILC (International Linear Collider) detector model for this study. The ILC ECAL is a sandwich structure between silicon sensors and tungsten radiators. We modified the geometry from the conventional analogue ECAL to the digital ECAL. The modified software is the ILC detector model MOKKA [1] version 6. The only difference except for the Si cell size is the Si sensitive thickness. In the conventional analogue ECAL, the sensitive Si thickness was for full volume of 500  $\mu\text{m}$  thickness. On the other hand, in the digital ECAL case, only the epitaxial layer's 15  $\mu\text{m}$  was used for the Si sensitive thickness. The rest of 485  $\mu\text{m}$  silicon thickness was implemented as non-sensitive silicon volume. Except for this Si sensitive thickness modification and for the cell size, all other geometry were kept as the same between the conventional ECAL case and the digital ECAL case as shown in Fig 1. (i.e. The W thickness, the plastic board thickness and total Si thickness were not changed at all.)

## Cell hit energy deposit

We compared the difference between single 20 GeV electrons in Fig 2 and single 20 GeV muons in Fig 3 by the cell hit energy deposit. As described there, the electron response have a muon-like minimum ionization peak. This means that the digital Ecal concept is possible in principle. In these figures, the lower energy bump is the cell boundary effect. It is because the path length of a secondary particle was shared by a few cells due to passing the cell boundary. This can be confirmed by checking the cell energy distributions between the isolated case in Fig 4 and the neighbour existed case in Fig 5. We also compared the different energy cases between the lower energy 1 GeV single electron case in Fig 6 and the higher energy 180 GeV single electron case in Fig 7. The shapes of cell energy deposit are almost same in these different incident energy cases. This also supports that the digital ECAL concept is possible to be realized indeed.

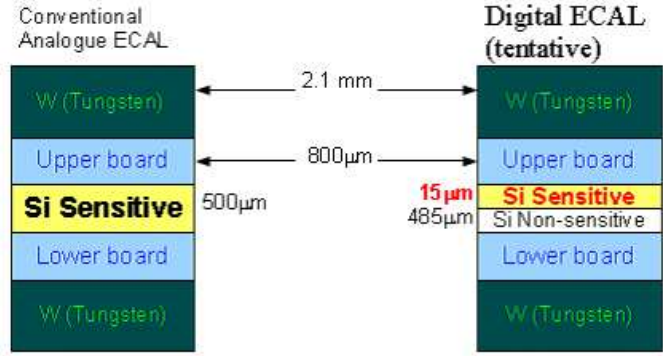


Figure 1: Geometry comparison between the analogue and the digital ECAL

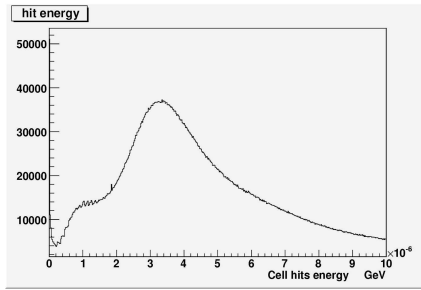


Figure 2: Cell hit energy deposit for 20 GeV single electron events with  $50 \mu\text{m} \times 50 \mu\text{m}$  cell

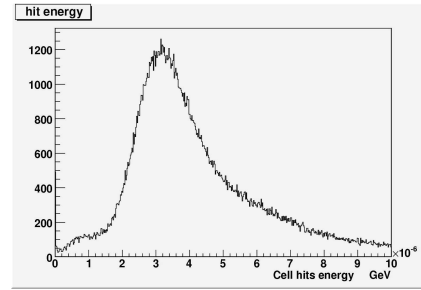


Figure 3: Cell hit energy deposit for 20 GeV single muon events with  $50 \mu\text{m} \times 50 \mu\text{m}$  cell

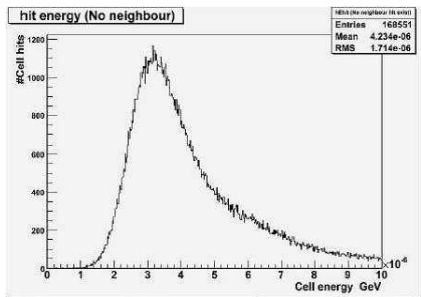


Figure 4: Cell hit energy deposit for the case that no neighbour hit exist. (In 20 GeV single muon events with  $50 \mu\text{m} \times 50 \mu\text{m}$  cell)

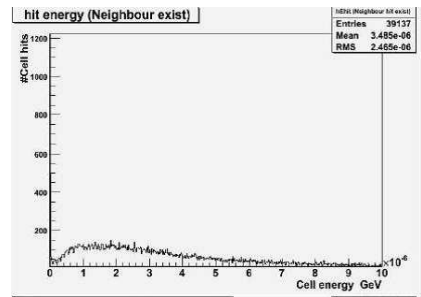


Figure 5: Cell hit energy deposit for the case that neighbour hits exist. (In 20 GeV single muon events with  $50 \mu\text{m} \times 50 \mu\text{m}$  cell)

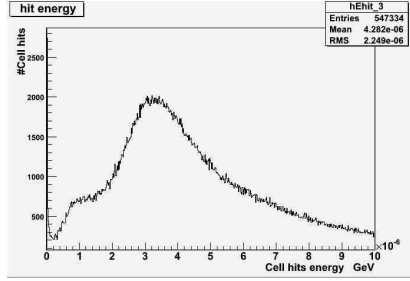


Figure 6: Cell hit energy deposit for 1 GeV single electron events with  $50 \mu\text{m} \times 50 \mu\text{m}$  cell

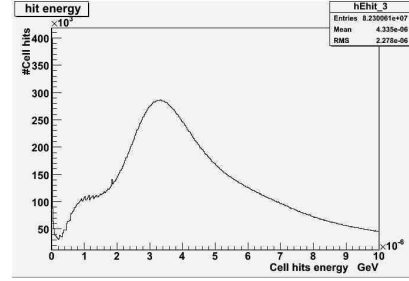


Figure 7: Cell hit energy deposit for 180 GeV single electron events with  $50 \mu\text{m} \times 50 \mu\text{m}$  cell

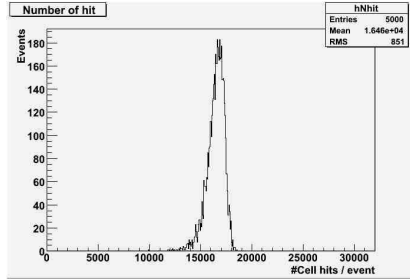


Figure 8: The raw number of cell hits per event. (In 180 GeV single electron events with  $50 \mu\text{m} \times 50 \mu\text{m}$  cell)

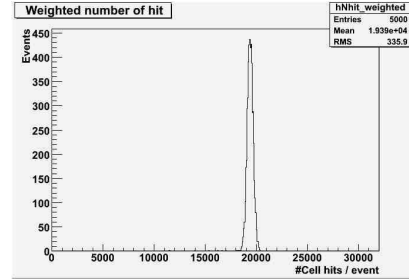


Figure 9: The wighted number of cell hits per event. (In 180 GeV single electron events with  $50 \mu\text{m} \times 50 \mu\text{m}$  cell)

## Geant4 Linearity

In the ILC detector model, the ECAL has 30 layers. Then the tungsten thickness is different between the inner layers and the outer layers. The tungsten thickness is 2.1 mm for the inner 20 layers and 4.2 mm for the outer 10 layers. This difference of the W thickness need be compensated when we counts the number of secondary particles. A weighted number which just doubled for outer layers works well. This can be confirmed in the comparison between the raw number case in Fig 8 and the weighted number case in Fig 9. The linearity for the weighted number of cell hits per event as a function of the incoming electron energy is shown in Fig 10. This is the linearity of the Geant4 response only which does not include any other realistic issues such as the charge diffusion, the digitization, the noise, the threshold and the dead area and so on.

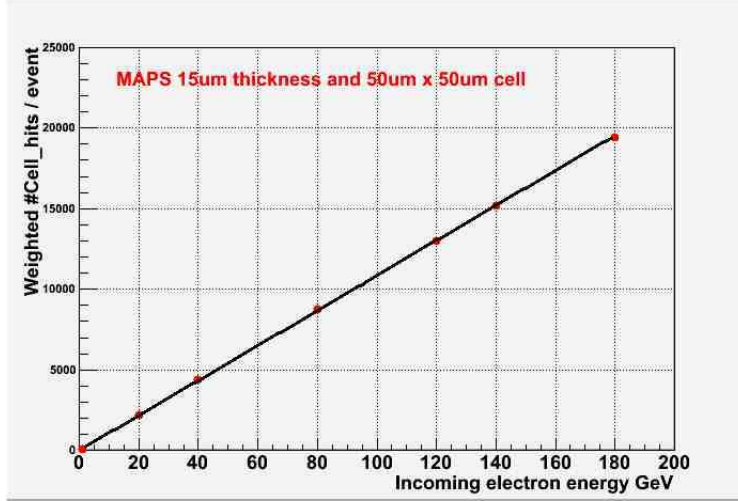


Figure 10: The weighted number of cell hits per event v.s. the incoming electron energy. ( $50 \mu\text{m} \times 50 \mu\text{m}$  cell)

## Cell size optimization

We compared the difference of cell size between  $25 \mu\text{m} \times 25 \mu\text{m}$  case in Fig 11,  $50 \mu\text{m} \times 50 \mu\text{m}$  case in Fig 12,  $100 \mu\text{m} \times 100 \mu\text{m}$  case in Fig 13 and  $400 \mu\text{m} \times 400 \mu\text{m}$  case in Fig 14 by the cell hit energy deposit distributions. They used 100 GeV single electron events. As described there, in the larger cell size case, the minimum ionization peak has a long Landau tail towards the larger cell hit energy deposit. This is because a single cell has several hits of secondary particles inside the one cell. On the other hand, in the smaller cell size case, the fraction of the cell boundary effect is increased. The linearity for the weighted number of cell hits as a function of the incident photon energy was compared between the  $50 \mu\text{m} \times 50 \mu\text{m}$  cell and the  $100 \mu\text{m} \times 100 \mu\text{m}$  cell in Fig 15. As described there, the linearity saturated at the high incident energy. The saturation is more severe in the larger cell size of  $100 \mu\text{m} \times 100 \mu\text{m}$  rather than the smaller cell size of  $50 \mu\text{m} \times 50 \mu\text{m}$ .

## Energy resolution

The energy resolution as a function of the incident electron energy is shown in Fig 16. Where the red mark is for the conventional analogue diode ECAL ( $1\text{cm} \times 1\text{cm}$  cell size, the energy is measured by the  $dE/dx$  times path lengths of secondary particles), the blue mark is for the digital ECAL  $50 \mu\text{m} \times 50 \mu\text{m}$  cell size without the cell neighbour clustering, the black mark is for the digital ECAL  $100 \mu\text{m} \times 100 \mu\text{m}$  cell size without the cell neighbour clustering and the

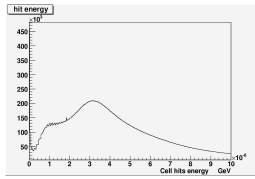


Figure 11: The cell hits energy deposit in 25  $\mu\text{m}$  x 25  $\mu\text{m}$  cell.

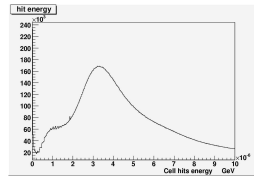


Figure 12: The cell hits energy deposit in 50  $\mu\text{m}$  x 50  $\mu\text{m}$  cell.

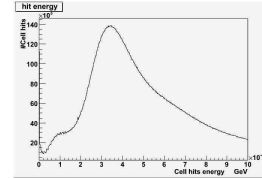


Figure 13: The cell hits energy deposit in 100  $\mu\text{m}$  x 100  $\mu\text{m}$  cell.

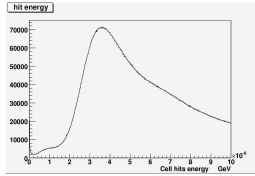


Figure 14: The cell hits energy deposit in 400  $\mu\text{m}$  x 400  $\mu\text{m}$  cell.

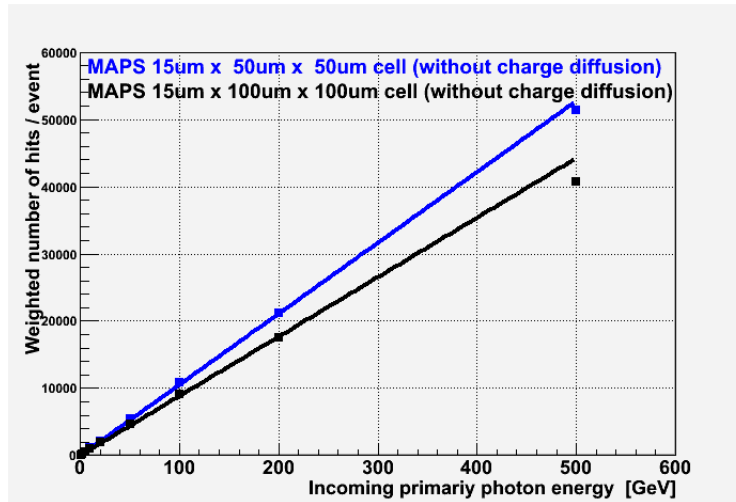


Figure 15: The weighted number of cell hits per event v.s. Incoming photon energy. With 50  $\mu\text{m}$  x 50  $\mu\text{m}$  cell (blue) and 100  $\mu\text{m}$  x 100  $\mu\text{m}$  cell (black).

green mark is the digital ECAL  $50\ \mu\text{m} \times 50\ \mu\text{m}$  cell size with the cell neighbour clustering. The cell neighbour clustering here is just summing up neighbour hits as one hit if some neighbour hits existed [2]. The general shape of the exponential falling down means that the higher resolution at the higher incident energy. This is because the high incident energy means the high statistics of secondary particles. Then the high statistics caused the low uncertainty. The difference between the  $50\ \mu\text{m} \times 50\ \mu\text{m}$  cell size and the  $100\ \mu\text{m} \times 100\ \mu\text{m}$  cell size both without the cell neighbour clustering is due to the cell boundary effect. The smaller cell size is more affected by the cell boundary. However, after the cell neighbour clustering, this effect is not problem anymore. The difference between the analogue diode ECAL and the digital ECAL with cell neighbour clustering will be due to the fluctuation of the path lengths of secondary particles. In the digital ECAL, the fluctuation component is basically the fluctuation of the number of secondary particles only. On the other hand, in the analogue diode case, the energy is measured by the  $dE/dx$  times the path length of secondary particle. This fluctuation of path length is an additional fluctuation component if it is compared with the digital ECAL. Thus, the digital ECAL can be better energy resolution than the conventional analogue diode ECAL. However, this study is based only on the Geant4 level. We have to consider other realistic things such as the charge diffusion, the noise, the threshold, the dead area and so on. These realistic issues are not included in this note. They are discussed in other place [2] [3] [4] [5].

## Summary

We investigated the possibility of the digital ECAL device by the Geant4 simulation. We tested fundamental things such as the cell size, the linearity and the resolution. We found that it is possible to realize the digital ECAL in principle. We also found that the digital ECAL has a potential of a slightly better energy resolution. However, for the real device, we need add other realistic issues in this Geant4 simulation study.

## Appendix: Consistency checks

As consistency checks, we compared the longitudinal shower shape in Fig 17 between the analogue diode ECAL and the digital ECAL. This used 100 GeV single photon events. The linearity slope for the energy deposit per event was also compared in Fig 18 between the analogue diode ECAL and the digital ECAL. The energy deposit for the digital ECAL is calculated by that the number of secondary particles times the mean value of the cell energy deposit. The mean value of the cell energy deposit is not the peak value of the minimum ionization peak. It includes the longer tail towards the higher energy deposit. In these figures, the single value 7.25 keV is used as the mean value of the cell energy deposit. The digital ECAL used the cell size of  $50\ \mu\text{m} \times 50\ \mu\text{m}$ . The analogue

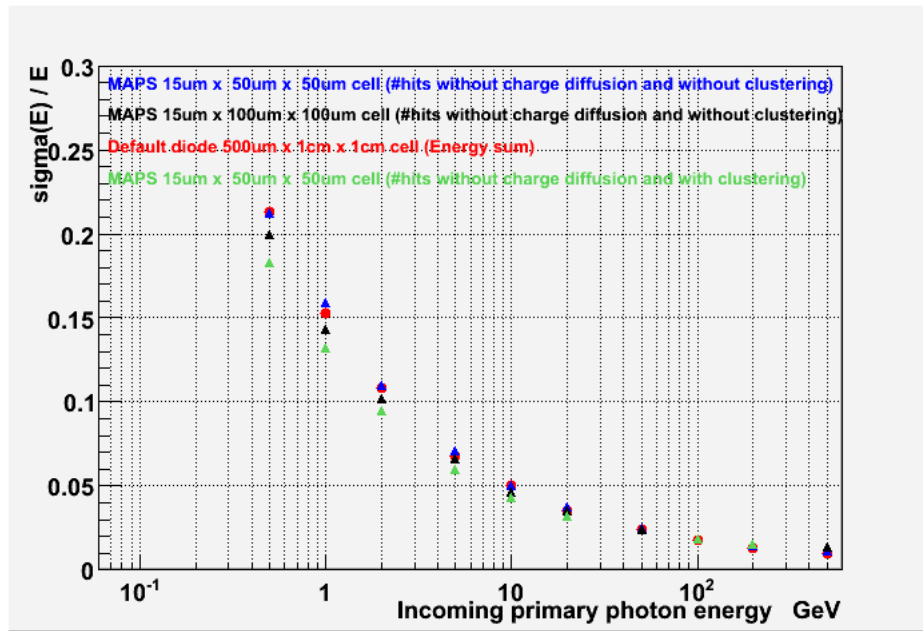


Figure 16: The energy resolution v.s. Incoming electron energy. In the analogue diode (red),  $50 \mu\text{m} \times 50 \mu\text{m}$  cell without the cell neighbour clustering (blue),  $100 \mu\text{m} \times 100 \mu\text{m}$  cell without cell neighbour clustering (black) and  $50 \mu\text{m} \times 50 \mu\text{m}$  cell with the cell neighbour clustering (green),



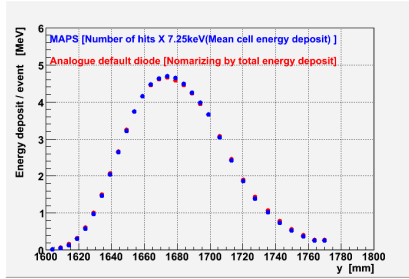


Figure 17: Longitudinal shower shape. The analogue diode ECAL (red) was normalized for the digital ECAL (blue). Each point corresponds to each layer.

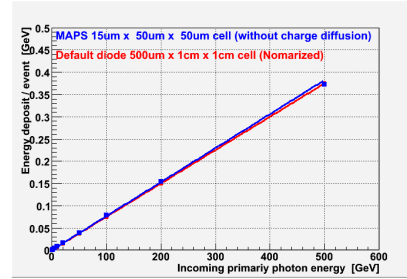


Figure 18: Energy deposit per event v.s. Incoming photon energy. The analogue ECAL (red) was normalized for the digital ECAL (blue).

diode was normalized into the digital ECAL by the factor of the Si sensitive thickness ratio  $15\mu\text{m}/500\mu\text{m} = 0.03$  in these figures. As described there, the analogue and the digital agree well both for the longitudinal shower shape and for the linearity slope. These agree with the expectations.

## References

- [1] [http://www-zeuthen.desy.de/linear\\_collider](http://www-zeuthen.desy.de/linear_collider)
- [2] A MAPS-based Digital Electromagnetic Calorimeter for the ILC: J.A. Ballin et al., arXiv:0709.1346v1, LCWS07 proceeding
- [3] A digital ECAL based on MAPS: J.A. Ballin et al., arXiv:0901.4457v1, LCWS08 proceeding
- [4] Monolithic Active Pixel Sensors (MAPS) in a Quadruple Well Technology for Nearly 100% Fill Factor and Full CMOS Pixels, J.A. Ballin et al., Sensors 2008, 8(9), 5336-5351
- [5] Design and performance of a CMOS study sensor for a binary readout electromagnetic calorimeter; J.A. Ballin et al., 2011 JINST 6 P05009